Journal of Inflammation Research

Dovepress
Taylor & Francis Group

Open Access Full Text Article

ORIGINAL RESEARCH

Identification of Senescence-Related Genes for the Prediction of Ulcerative Colitis Based on Interpretable Machine Learning Models

Jingjing Ma[1,*], Chen Chen[2,3,*], Nian Wang[1], Ting Fang[1], Yinghui Liu[1], Pengzhan He[1], Weiguo Dong[4]

[1]Department of Geriatric, Renmin Hospital of Wuhan University, Wuhan, Hubei, 430060, People's Republic of China; [2]Department of General Surgery, Renmin Hospital of Wuhan University, Wuhan, People's Republic of China; [3]General Surgery Laboratory, Renmin Hospital of Wuhan University, Wuhan, People's Republic of China; [4]Department of Gastroenterology, Renmin Hospital of Wuhan University, Wuhan, Hubei, 430060, People's Republic of China

*These authors contributed equally to this work

Correspondence: Weiguo Dong, Department of Gastroenterology, Renmin Hospital of Wuhan University, No. 99 Zhangzhidong Road, Wuhan, Hubei Province, 430060, People's Republic of China, Tel +027-88041911, Email dongweiguo@whu.edu.cn

Background: Cellular senescence, a hallmark of aging, significantly contributes to the pathology of ulcerative colitis (UC). Despite this, the role of senescence-related genes in UC remains largely undefined. This study seeks to clarify the impact of cellular senescence on UC by identifying key senescence-related genes and developing diagnostic models with potential clinical utility.

Methods: Clinical data and gene expression profiles were obtained from the Gene Expression Omnibus (GEO) database. Senescence-related differentially expressed genes (sene-DEGs) between patients with UC and healthy controls were identified using various bioinformatics techniques. Functional enrichment and immune infiltration analyses were performed to understand subtype characteristics derived from sene-DEGs through consensus clustering. Machine learning algorithms were employed to select feature genes from sene-DEGs, and their expression was validated across multiple independent datasets and human specimens. A nomogram incorporating these feature genes was created and assessed, with its diagnostic performance evaluated using receiver operating characteristic (ROC) analysis on independent datasets.

Results: Fourteen senescence-related differential genes were identified between patients with UC and healthy controls. These genes enabled the classification of patients with UC into molecular subtypes via unsupervised clustering. ABCB1 and LCN2 emerged as central hub genes through machine learning and feature importance analysis. ROC analysis verified their diagnostic value across various datasets. Validation in independent datasets and human specimens supported the bioinformatics findings. Furthermore, the expression levels of ABCB1 and LCN2 showed significant associations with immune cell profiles. The logistic regression (LR) model based on these genes demonstrated accurate UC prediction, as confirmed by ROC curve analysis. The nomogram model, constructed with feature genes, exhibited outstanding prediction capabilities, supported by DCA, C index, and calibration curve assessments.

Conclusion: This integrated bioinformatics approach identified ABCB1 and LCN2 as significant biomarkers associated with cellular senescence. These findings enhance the understanding of cellular senescence in UC pathogenesis and propose its potential as a valuable diagnostic biomarker.

Keywords: ulcerative colitis, cellular senescence, biomarkers, diagnostic model, machine learning

Introduction

Ulcerative colitis (UC), a chronic and recurrent inflammatory bowel disease (IBD), primarily affects the colon and rectum with diffuse, superficial inflammation. Common symptoms include chronic diarrhea, bloody stools, abdominal pain, and weight loss.[1,2] The incidence and prevalence of UC have been rising globally,[3] and patients with long-term UC face an elevated risk of colorectal cancer, with a steady annual increase of 0.5%-1% after 10 years.[4,5] UC poses

Received: 10 December 2024
Accepted: 5 March 2025
Published: 10 March 2025

a significant threat to public health and incurs considerable economic costs. Therefore, a deep understanding of UC's pathological and molecular characteristics is essential for advancing research and improving clinical management.

The exact etiology of UC is still not fully understood, involving a complex interplay of environmental factors, genetics, infectious agents, gut microbiota, immune dysregulation, and intestinal epithelial damage.[6,7] Cellular senescence, a major driver of aging and age-related diseases, is triggered by DNA damage, telomere attrition, and oxidative stress. Recent research has highlighted a complex interplay between inflammation and senescence.[8,9] Senescent cells release various bioactive molecules that exacerbate inflammation and promote senescence in surrounding cells. Conversely, inflammation can accelerate immune cell senescence, impairing immune function. Notably, the accumulation of DNA damage in the colonic tissue of patients with UC is a significant marker of aging.[10] Additionally, studies have identified a novel link between intestinal cellular senescence and colonic inflammation. For instance, *Fusobacterium nucleatum*-Exo has been shown to induce DNA damage and cellular senescence through the TIMELESS-mediated senescence pathway, while short telomeres have been observed in the colonic mucosa of UC models.[11] Despite advancements in understanding inflammation and cellular senescence, their interrelationship remains poorly elucidated.

This study aims to clarify the role of cellular senescence in UC by identifying key senescence-related genes and developing diagnostic models with potential clinical applications.

Materials and Methods

Data Acquisition and Pre-Processing

Gene expression data and associated clinical information were retrieved from the Gene Expression Omnibus (GEO) database (http://www.ncbi.nlm.nih.gov/geo). For this analysis, a dataset of 866 senescence-related genes from the CellAge database (https://genomics.senescence.info/cells/) was employed, with the complete list available in Supplementary Table S1.

Differential Gene Expression Analysis and Functional Analysis

Differentially expressed genes (DEGs) between patients with UC and healthy controls (HC) were identified using the "limma" R package. Graphical representations of the results were generated using the "ggplot2" and "pheatmap" R packages. Kyoto Encyclopaedia of Genes and Genomes (KEGG) and Gene Ontology (GO) enrichment analyses were conducted with the "clusterProfiler" and "org.Hs.eg.db" R packages, applying a q-value threshold of < 0.05 to elucidate the biological mechanisms underlying the DEGs.[12] The senescence-related DEGs (sene-DEGs) were identified by intersecting DEGs with senescence-related genes.

The sene-DEGs were submitted to the STRING database (https://cn.string-db.org) for protein-protein interaction (PPI) network construction, with a confidence level set at 0.4. Visualization was performed using Cytoscape 3.9.1. The diagnostic potential of the sene-DEGs for UC was assessed through receiver operating characteristic (ROC) analysis using the "pROC" R package.

Assessment of Immune Infiltration Patterns in UC

Single-sample Gene Set Enrichment Analysis (ssGSEA) was employed to evaluate immune cell infiltration levels in the colon tissue of patients with UC compared to HC.

Identification of Feature Biomarkers Using Machine Learning Algorithms

The analysis used a training set of 193 samples (32 hC and 161 patients with UC). We applied eight different machine learning algorithms—AdaBoost, LightGBM, Decision Trees (DT), XGBoost, Random Forest (RF), K-Nearest Neighbors (KNN), Naïve Bayes, and Support Vector Machines (SVM)—using gene expression data as variables. To optimize the performance of the algorithm, we employed a systematic parameter tuning process. The final parameters were selected based on their ability to maximize mean squared error while minimizing potential overfitting, as validated through 10-fold cross-validation. The sensitivity analyses were also conducted to ensure the robustness of the selected parameters across varying subsets of the data.

Performance of the algorithms was evaluated on a testing set by measuring accuracy, F1 score, precision, sensitivity, specificity, and kappa. Additionally, the area under the ROC curve (AUC) was computed to assess the discriminative power between HC and patients with UC. The implementations were as follows: AdaBoost, DT, and KNN were executed using the R package "caret"; RF was performed with "ranger"; LightGBM was run with "lightgbm" and "tidymodels"; XGBoost was handled by "xgboost"; Naïve Bayes and SVM were processed using "e1071"; and model interpretation was conducted with "DALEX".

Construction and Evaluation of Binary Logistic Regression Model

To determine the matching coefficients of senescence-related DEGs and compute a risk score for each sample, we utilized a binary logistic regression (LR) model. The "rms" package was employed to create the nomogram. The performance of the risk scores was assessed through decision curve analysis (DCA), calibration curve analysis, and AUC calculations. Model generalizability was tested using the GSE59071 dataset from the GEO database.

Unsupervised Clustering of Patients with UC and Functional Enrichment Analysis

Unsupervised clustering analysis was performed using the "ConsensusClusterPlus" R package.[13] The k-means clustering method was executed 1000 times with a maximum number of subtypes set to k = 6. The optimal number of subtypes was determined by evaluating the cumulative distribution function (CDF) curve, consensus matrix, and consistent cluster score.

Gene Set Variation Analysis (GSVA) was conducted using the "GSVA" R package[14] to compare enriched functions and pathways across different mitophagy-related subtypes. The analysis utilized gene sets "c2.cp.kegg.v7.4.symbols" and "c5.go.bp.v7.5.1.symbols" from the MSigDB database. Routes and functions with significant enrichment were identified by GSVA scores with |t| values greater than two.

Immunohistochemistry (IHC)

Colon biopsies from patients diagnosed with UC and HC were collected at the Department of Pathology, Renmin Hospital of Wuhan University, with basic information shown in Supplementary Table S2. Paraffin-embedded tissue slices were deparaffinized and rehydrated. The antigen retrieval process was carried out using citrate buffer. To suppress any endogenous peroxidase activity, the sections were immersed in a 0.3% hydrogen peroxide solution for 10 minutes. Subsequently, the tissue slices were incubated with a blocking solution of 5% bovine serum albumin (BSA), followed by the primary antibody incubation overnight at 4°C, washing it with PBS afterward. Apply the incubation with secondary antibodies at room temperature, followed by a PBS wash. Perform DAB staining and stop the reaction with distilled water, counterstaining with hematoxylin afterward. The slices were scrutinized under light microscopy to assess the results. The primary antibodies used in this process were ABCB1 (Cat No. A11758) and LCN2 (Cat No. 26991-1-AP).

The study adhered to the Declaration of Helsinki and was approved by the Ethics Committee of Renmin Hospital of Wuhan University (WDRY2021-K025). Informed consent was obtained from all patients, and the study was conducted in accordance with relevant guidelines and regulations.

Statistical Analysis

Statistical analyses were performed using R version 4.2.3 (https://www.r-project.org). Comparisons between two groups were conducted using the *t*-test, while *ANOVA* was used for comparisons involving three or more groups. *Spearman* correlation analysis was carried out using the "ggpubr" and "stats" R packages. Statistical significance was defined as a *p*-value or adjusted *p*-value of less than 0.05.

Results

Data Preprocessing and Identification of Senescence-Related DEGs

Gene expression profiles from colonic tissues of 161 patients with UC and 32 hC, extracted from datasets GSE87466 and GSE75214, were analyzed. Initial clustering by dataset rather than sample type on the principal component dimension

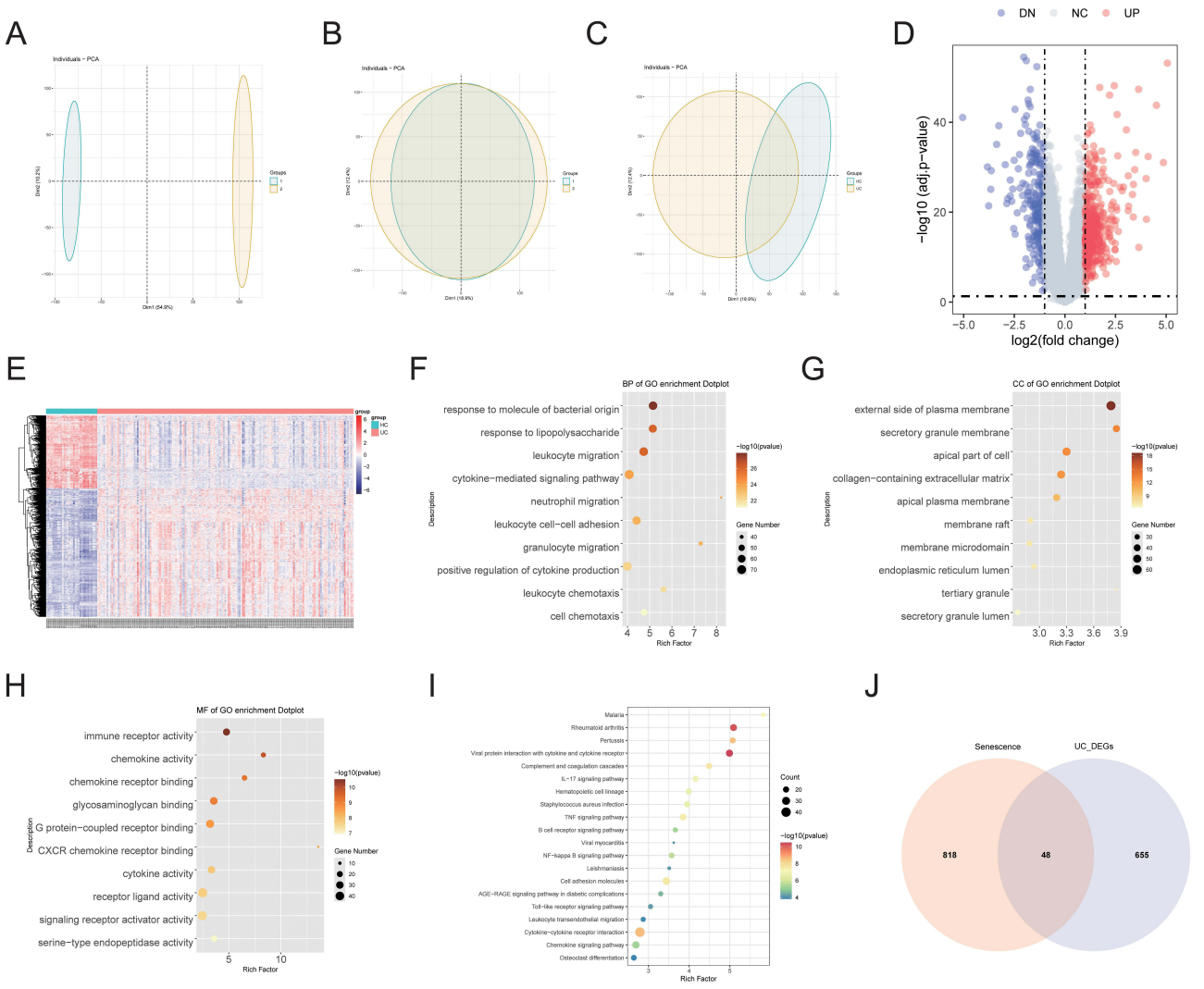

Figure 1 Identification of sene-DEGs. (**A** and **B**) PCA of two datasets before (**A**) and after (**B**) batch effect correction. (**C**) PCA of the merged dataset. (**D** and **E**) Volcano plot (**D**) and heatmap (**E**) revealing gene expression patterns between patients with UC and HC. (**F**) GO BP enrichment analysis of sene-DEGs. (**G**) GO CC enrichment analysis of sene-DEGs. (**H**) GO MF enrichment analysis of sene-DEGs. (**I**) KEGG pathway enrichment analysis of sene-DEGs. (**J**) Venn diagram showing overlap between DEGs and senescence-related genes.

Abbreviations: PCA, principal component analysis; UC, ulcerative colitis; HC, healthy controls; KEGG, the Kyoto Encyclopedia of Genes and Genomes analyses; GO, the Gene Ontology.

revealed a predominant batch effect, with data source impact overshadowing sample type (Figure 1A). Following batch correction, samples clustered predominantly by UC status versus HC, demonstrating that sample type was the primary factor influencing variation (Figure 1B and C). Post-correction analysis identified 703 DEGs (Figure 1D and E). Functional enrichment and KEGG pathway analyses were performed on the key targets. Biological process (BP) enrichment primarily involved responses to bacterial molecules and lipopolysaccharides, as well as leukocyte and neutrophil migration, and cytokine-mediated signaling pathways (Figure 1F). Cellular component (CC) enrichment was noted in the external side of the plasma membrane, secretory granule membrane, apical part of the cell, and collagen-containing extracellular matrix (Figure 1G). Molecular function (MF) enrichment focused on immune receptor activity, chemokine activity, and chemokine receptor binding (Figure 1H). The top 20 metabolic pathways highlighted in KEGG analysis included IL-17 signaling, TNF signaling, and NF-kappa B signaling pathways (Figure 1I).

To elucidate the role of senescence in UC development, DEGs were intersected with a list of 866 senescence-related genes, resulting in 48 senescence-related DEGs (sene-DEGs) (Figure 1J). These genes were analyzed in the STRING database to construct a PPI network (Figure 2A). Gene clusters were identified using the MCODE plugin, focusing on the

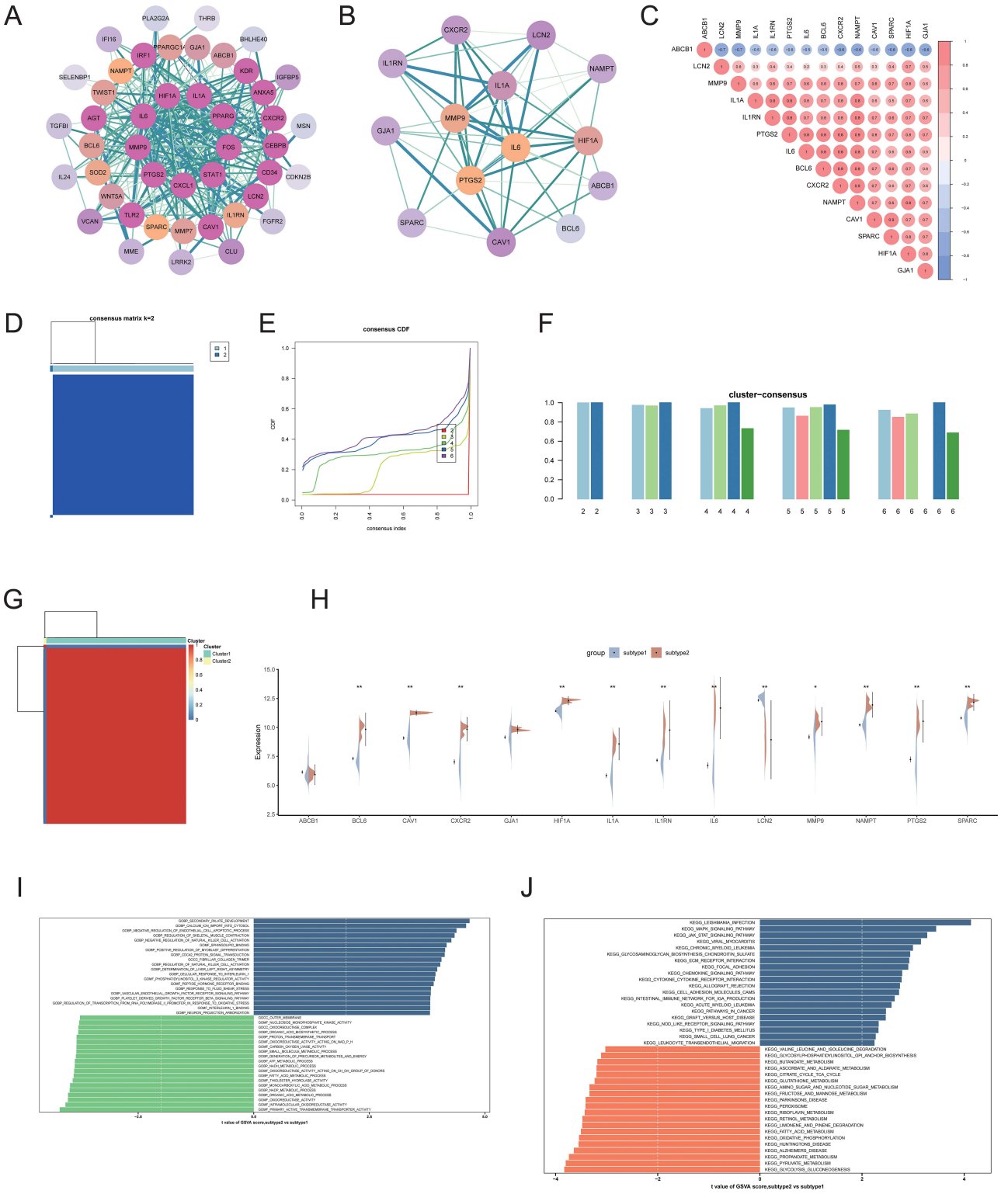

Figure 2 Analysis of sene-DEGs. and subtype classification. (**A**) PPI network of 48 sene-DEGs. (**B**) MCODE sub-network analysis. (**C**) Correlation heatmap of 14 sene-DEGs. (**D**) Consensus clustering matrix for k = 2. (**E**) Consensus CDF curves for k = 2 to 6. (**F**) Consensus scores for each subtype from k = 2 to 6. (**G**) Heatmap showing gene expression patterns across subtypes. (**H**) Split violin plot showing expression levels of 14 sene-DEGs between subtypes. (**I** and **J**) Differences in enriched biological functions (**I**) and hallmark pathways (**J**) between subtypes, ranked by GSVA scores. *$p < 0.05$, **$p < 0.01$.

https://doi.org/10.2147/JIR.S508396

highest-scoring module. A correlation analysis of the 14 genes within this module was conducted to assess senescence' s role in UC progression (Figure 2B). Additionally, the gene relationship network diagram revealed significant interconnections among the sene-DEGs, indicating a strong synergy among these senescence-related genes (Figure 2C).

Construction of Senescence Subtypes in UC

Based on the fourteen sene-DEGs, an unsupervised clustering analysis divided patients with UC into two distinct subtypes, 1 and 2 (Figure 2D-F). Heatmap analysis highlighted significant differences in gene expression profiles between these subtypes (Figure 2G). While variations in the expression levels of the fourteen sene-DEGs were notable, differences in ABCB1 and GJA1 expression did not reach statistical significance (Figure 2H).

GSVA was performed to explore differences in functional and pathway enrichment between the two subtypes. Subtype 1 exhibited upregulation in pathways related to primary active transmembrane transporter activity, intramolecular oxidoreductase activity, oxidoreductase activity, organic acid metabolism, NADP metabolism, monocarboxylic acid metabolism, thiolester hydrolase activity, and fatty acid metabolism. Conversely, subtype 2 showed upregulation in pathways such as secondary palate development, calcium ion import into the cytosol, negative regulation of endothelial cell apoptosis, regulation of skeletal muscle contraction, negative regulation of natural killer cell activation, and sphingolipid binding (Figure 2I).

KEGG pathway analysis further revealed that subtype 1 had upregulated metabolic pathways including glycolysis and gluconeogenesis, pyruvate metabolism, propanoate metabolism, oxidative phosphorylation, fatty acid metabolism, and limonene and pinene degradation. In contrast, subtype 2 exhibited elevated pathways associated with MAPK signaling, JAK/STAT signaling, ECM receptor interaction, and chemokine signaling (Figure 2J).

Distinct Immune Patterns Between Senescence-Related UC Subgroups

Immune factors play a pivotal role in UC, and cellular senescence, a significant driver of aging and age-related diseases, is central to UC pathology. The interaction between inflammation and senescence forms a complex, self-perpetuating cycle.[8,9] To elucidate the relationship between cellular senescence and immune function in patients with UC, immune cell distribution and activity were analyzed across subtypes 1 and 2 (Figure 3A). Differences in immune cell quantities and correlations among the 28 immune cell types are illustrated in Figure 3B and C. Subtype 1 exhibited higher infiltration of activated dendritic cells, CD56 bright natural killer cells, central memory CD8 T cells, immature dendritic cells, memory B cells, plasmacytoid dendritic cells, type 17 T helper cells, and type 2 T helper cells. In contrast, subtype 2 showed increased presence of eosinophils, mast cells, myeloid-derived suppressor cells (MDSCs), and regulatory T cells (Figure 3C).

Further analysis of immune-related gene expression revealed that immune checkpoint-associated genes, including CD27, CD40, CD86, CTLA4, and HAVCR2, were significantly upregulated in subtype 2. This suggests that subtype 1, associated with senescence, might benefit more from immune-based therapies (Figure 3D). Additionally, most immune activation-related genes (Figure 3E) and immunosuppression-related genes (Figure 3F) were upregulated in subtype 2, indicating a more pronounced immune response compared to subtype 1.

Identification of Feature Biomarkers Using Machine Learning Algorithms

A variety of machine learning algorithms—AdaBoost, Naïve Bayes, DT, KNN, LightGBM, RF, SVM, and XGBoost—were utilized to identify feature genes associated with UC. Performance metrics for each algorithm are summarized in Table 1. All models achieved recall rates exceeding 50%. ROC curves and importance plot of fourteen genes for each algorithm were depicted in Figure 4A-H. Among these, LightGBM achieved the highest AUC value of 0.978, whereas AdaBoost excelled with the highest accuracy (0.8426), kappa (0.4894), and F1-score (0.9040).

Construction and Evaluation of the LR Model

Based on the variable importance analysis, the final set of characteristic genes was identified by selecting the top five sene-DEGs common to both LightGBM and AdaBoost: ABCB1, LCN2, and HIF1A. The logistic regression (LR) model was constructed using these genes, with the final risk score calculated as (−1.9777 * ABCB1) + (1.0733 * LCN2). The nomogram generated from

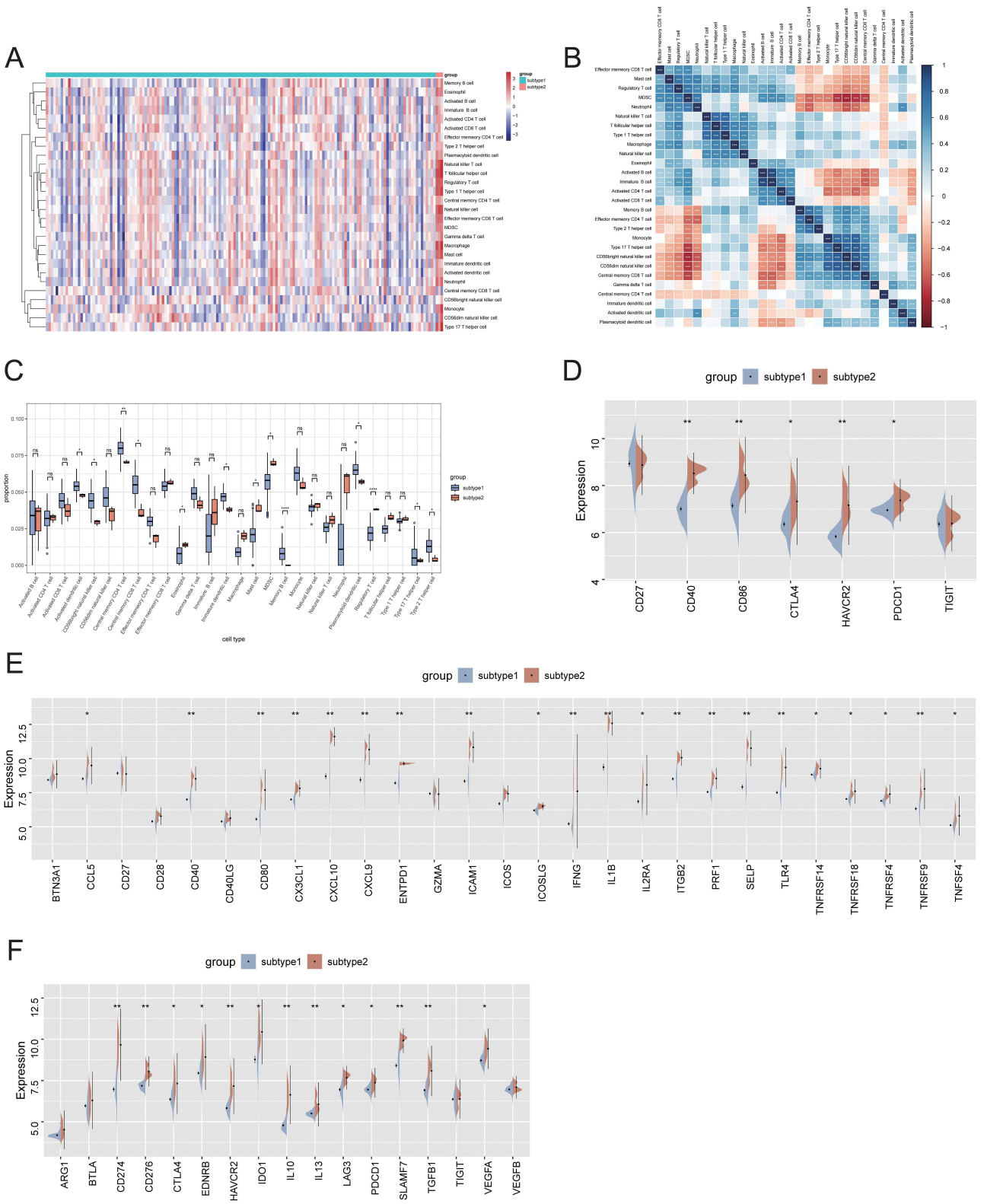

Figure 3 Immune cell distribution and activity in UC subtypes. (**A**) Heatmap of immune cell infiltration between subtypes 1 and 2. (**B**) Heatmap showing correlations between 28 immune cell types. (**C**) Boxplot depicting differences in immune cell infiltration between subtypes. (**D-F**) Split violin plots showing expression levels of immune checkpoint genes (**D**), immune activation genes (**E**), and immune suppression genes (**F**) between subtypes. *$p < 0.05$, **$p < 0.01$, ***$p < 0.001$, ****$p < 0.0001$.
Abbreviation: ns, not statistically significant.

https://doi.org/10.2147/JIR.S508396

Table 1 Comparison of the Diagnostic Efficacy Among Eight Distinct Machine Learning Models

ML Algorithms	Accuracy	Kappa	Sensitivity	Specificity	Precision	Recall	F1	AUC
Decision Tree	0.6759	0.2652	1	0.2391	0.6392	1	0.7799	0.820
SVM	0.8148	0.4395	1	0.3548	0.7938	1	0.8851	0.969
Naïve Bayes	0.787	0.3959	1	0.3235	0.7629	1	0.8655	0.961
LightGBM	0.8241	0.4554	1	0.3667	0.8041	1	0.8914	0.978
Random Forest	0.7963	0.4098	1	0.3333	0.7732	1	0.8721	0.978
KNN	0.8148	0.4395	1	0.3548	0.7938	1	0.8851	0.968
Adaboost	0.8426	0.4894	1	0.3929	0.8247	1	0.9040	0.972
XGBoost	0.8333	0.472	1	0.3793	0.8144	1	0.8977	0.972

the LR model for the training set is depicted in Figure 5A. As illustrated in Figure 5B, patients with UC exhibited significantly higher risk scores compared to HC in the training set. The model's fit was validated with 1000 bootstrap samples, and calibration curves (Figure 5C) confirmed the LR model's robust predictive accuracy. Decision Curve Analysis (DCA) consistently demonstrated that the model's predictions provide clinical benefit to patients with UC, with the model-based decision curve remaining above the reference line (Figure 5D). The model achieved an AUC of 0.985 through 10-fold cross-validation (Figure 5E). Additionally, the calibration and DCA curves for the testing set also indicated strong diagnostic performance (Figures 5F and G), with an AUC of 0.979 (Figure 5H). And the risk scores of UC patients were substantially greater than those of healthy controls in the testing set (Figure 5I).

Verification of Feature Biomarkers and Effectiveness Evaluation

ROC analysis of the training set revealed AUC values of 0.971 for ABCB1 and 0.954 for LCN2 (Figure 6A and B), indicating their effective diagnostic potential for UC. The GSE59071 dataset, used for testing, confirmed that patients with UC had elevated LCN2 expression and reduced ABCB1 levels (Figure 6C). In this set, AUC values for ABCB1 and LCN2 were 0.978 and 0.928, respectively (Figure 6D and E). External validation with the GSE206285 dataset also demonstrated that patients with UC exhibited higher LCN2 and lower ABCB1 expression levels (Figure 6F). The AUC values for this validation were 0.981 for ABCB1 and 0.882 for LCN2 (Figure 6G and H).

Analysis of diseased colonic tissues from patients with active UC showed increased LCN2 and decreased ABCB1 levels compared to non-inflammatory tissues (Figure 6I). Additionally, LCN2 levels were significantly higher in patients with active UC compared to those with inactive UC, while ABCB1 expression did not show statistically significant variation (Figure 6J).

Human tissue validation further supported these results, with ABCB1 significantly downregulated and LCN2 significantly upregulated in UC colonic tissues (Figure 7A and B).

Association Between Colonic Mucosal Invasion of Active UC and Senescence

Biologics, including TNF-α inhibitors such as golimumab (GLM) and IL-12/IL-23 inhibitors like ustekinumab (Ust), are established as first-line treatments for moderate to severe UC. The impact of these biologics on cellular senescence was evaluated using the GSE92415 and GSE206285 datasets.

Prior to Ust treatment, no significant differences in ABCB1 and LCN2 expression were observed between the mucosal healing group and non-responders (Figure 8A). Moreover, the baseline expression patterns of ABCB1 and LCN2 in patients with UC responding to Ust were similar to those in non-responders (Figure 8B).

For GLM treatment, ABCB1 expression was notably lower in patients with active UC compared to HC, while LCN2 levels were significantly elevated (Figure 8C). Post-treatment with GLM, there was a marked increase in ABCB1 expression and a reduction in LCN2 levels among the clinical response group (Figure 8D).

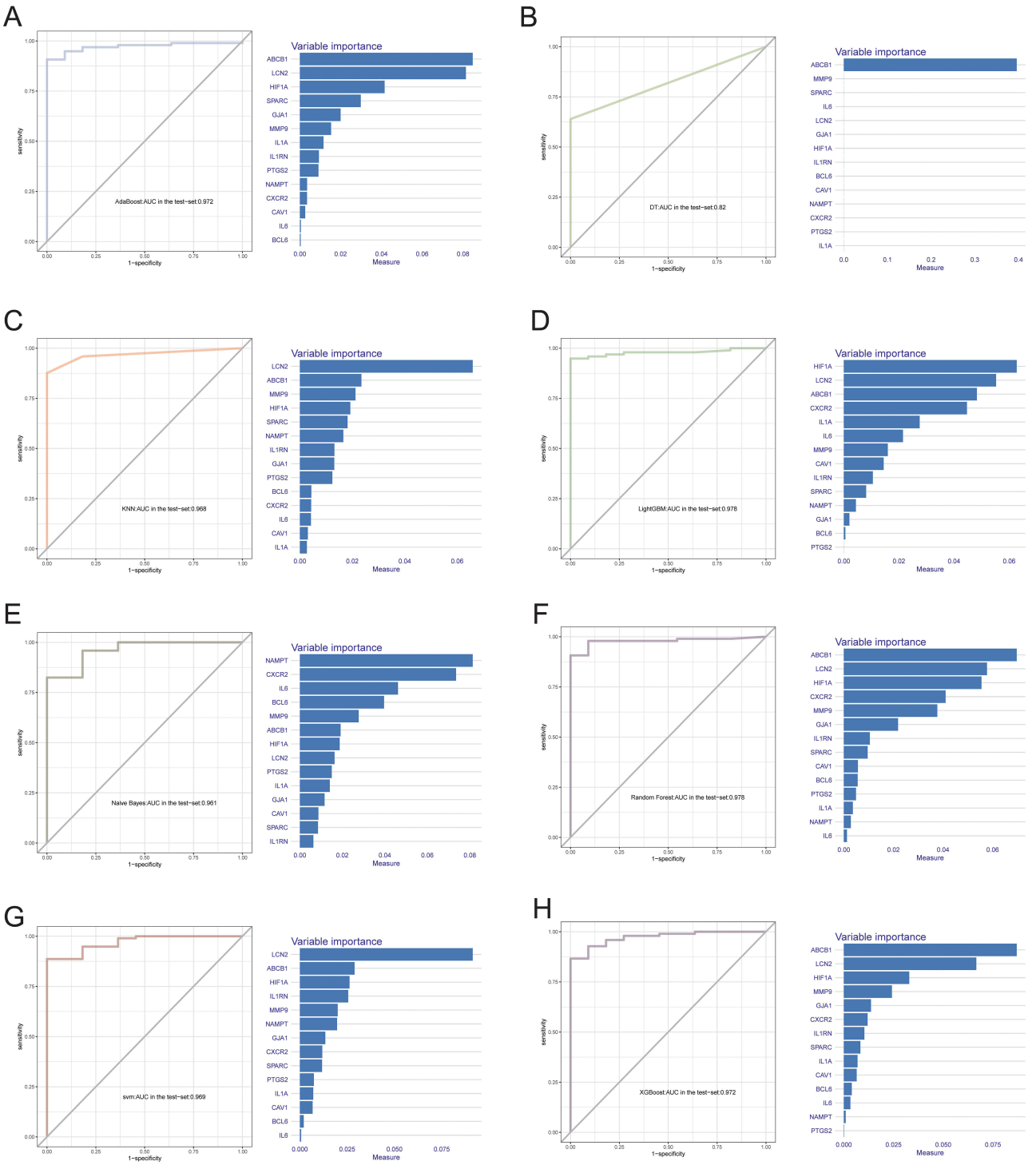

Figure 4 Evaluation of the eight machine learning algorithms based on the area under the ROC curve (AUC) and variable importance plot of fourteen genes. (**A**) AdaBoost. (**B**) Decision Tree. (**C**) KNN. (**D**) LightGBM. (**E**) Naïve Bayes. (**F**) Random Forest. (**G**) SVM. (**H**) XGBoost.
Abbreviations: KNN, K-nearest neighbors; LightGBM, Light Gradient Boosting; SVM, support vector machines; XGBoost, eXtreme Gradient Boosting.

Immune-Infiltrating Landscape of Patients with UC

To further understand the immune microenvironment in UC, the distribution and activity of immune cells were analyzed. The immune cell distribution in both patients with UC and HC is depicted in Figure 9A. Figure 9B presents the correlations among 28 immune cell types, and Figure 9C highlights the differences in immune cell quantities between the

https://doi.org/10.2147/JIR.S508396

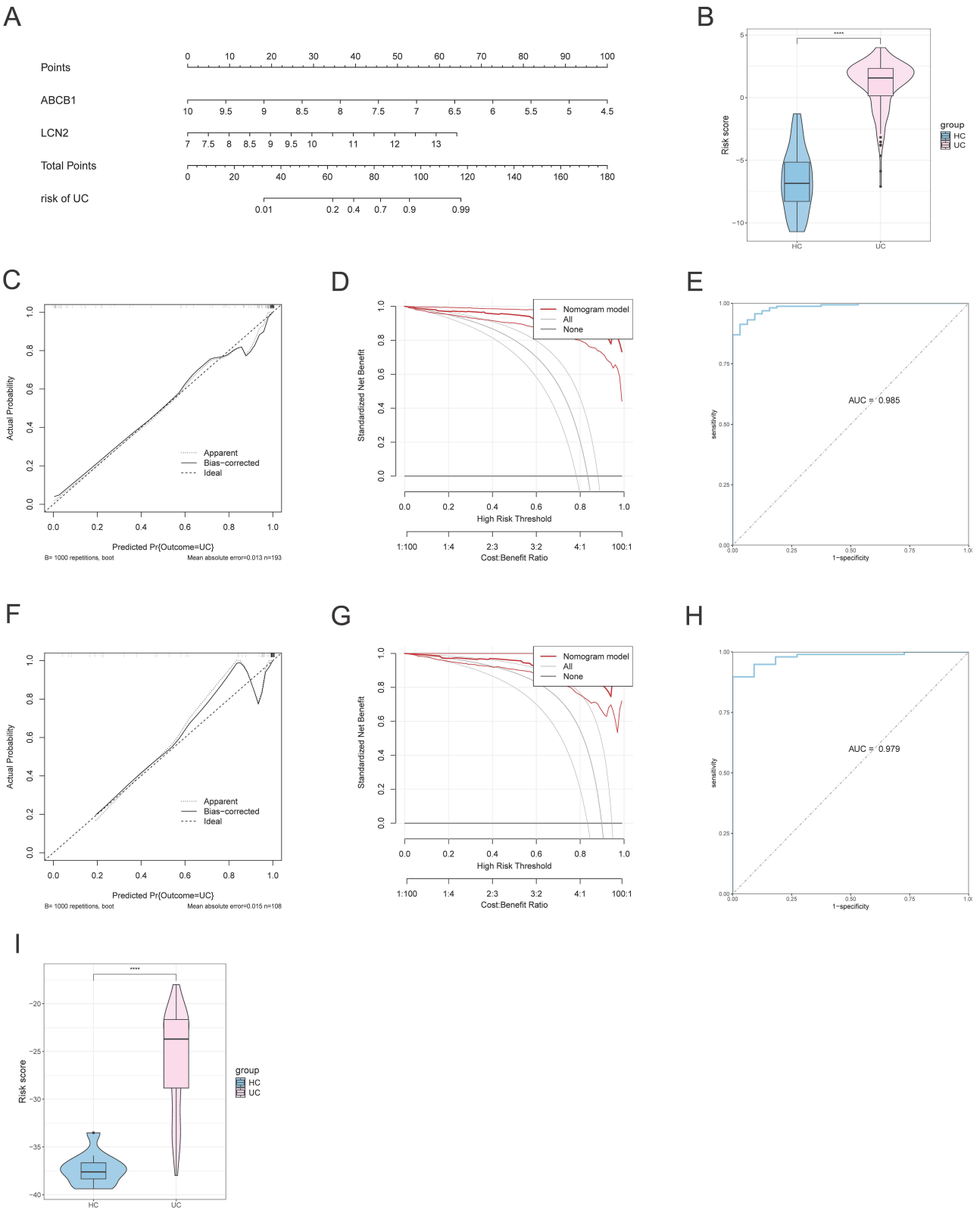

Figure 5 Construction and evaluation of the UC risk nomogram. (**A**) Development of a nomogram to predict UC risk using ABCB1 and LCN2 within the training set. (**B**) Comparison of risk distributions between patients with UC and HC within the training set. (**C**) The calibration curve assessed the nomogram's predictive accuracy in the training set. (**D**) DCA determined the nomogram's clinical benefit within the training set. (**E**) ROC curves assessed the model's diagnostic performance in the training set. (**F**) The calibration curve evaluated the nomogram's prediction accuracy in the testing set. (**G**) DCA determined the nomogram's clinical benefit within the testing set. (**H**) ROC curves assessed the model's diagnostic performance in the testing set. (**I**) Comparison of risk distributions between patients with UC and HC in the testing set. ****$p < 0.0001$.

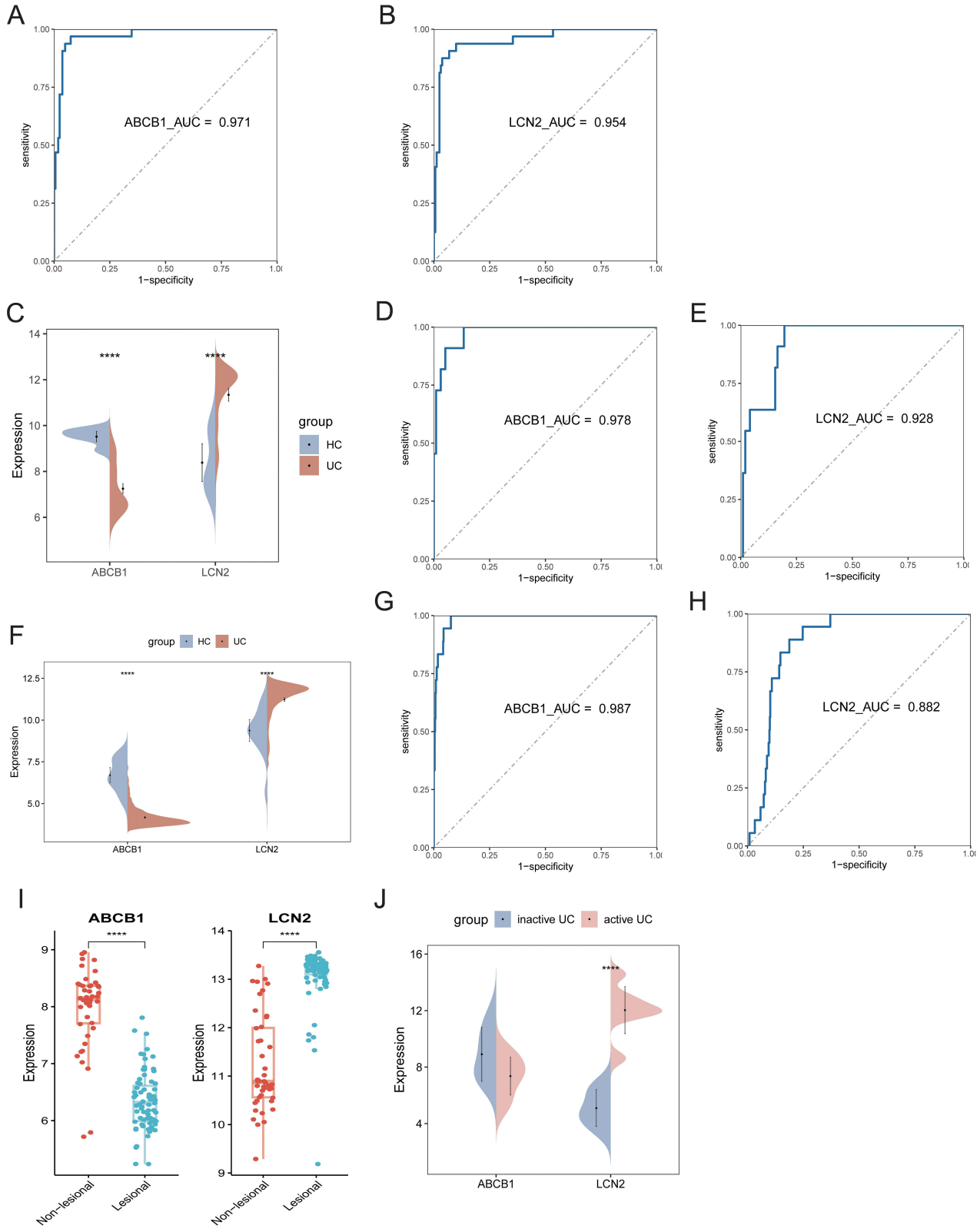

Figure 6 Diagnostic performance and expression levels of ABCB1 and LCN2. (**A** and **B**) ROC curves assessed the diagnostic performance of ABCB1 (**A**) and LCN2 (**B**) in the training set. (**C**) Comparison of ABCB1 and LCN2 expression levels between patients with UC and HC in the testing set. (**D** and **E**) ROC curves evaluated the diagnostic performance of ABCB1 (**D**) and LCN2 (**E**) in the testing set. (**F**) Comparison of ABCB1 and LCN2 expression levels between patients with UC and HC in the GSE206285 dataset. (**G** and **H**) ROC curves assessed the diagnostic performance of ABCB1 (**G**) and LCN2 (**H**) in the GSE206285 dataset. (**I**) Comparison of ABCB1 and LCN2 expression levels between non-lesional and lesional UC individuals. (**J**) Comparison of ABCB1 and LCN2 expression levels between inactive and active UC individuals. ****$p < 0.0001$.

https://doi.org/10.2147/JIR.S508396

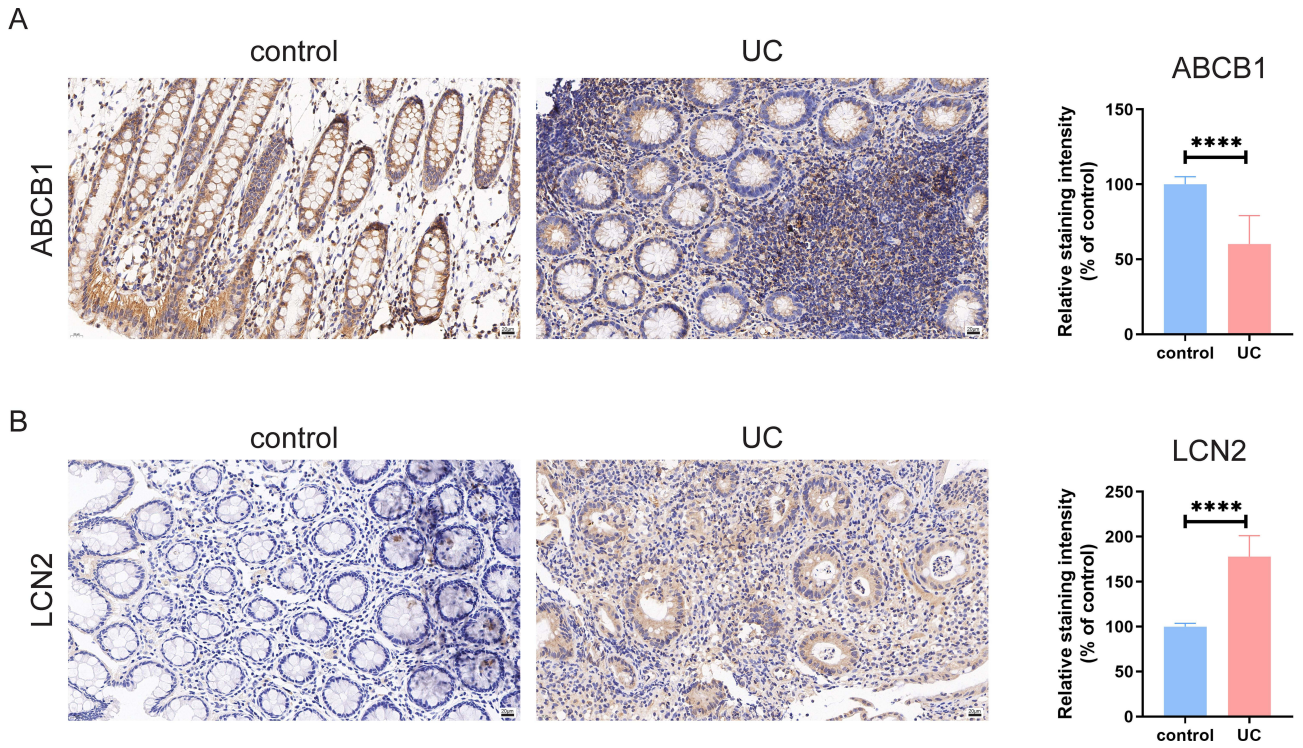

Figure 7 Immunohistochemical analysis of ABCB1 and LCN2 expression. (**A**) Immunohistochemistry and quantitative assessment of ABCB1 expression in patients with UC and HC. Original magnification: 400×, scale bar = 50 μm. (**B**) Immunohistochemistry and quantitative assessment of LCN2 expression in patients with UC and HC. Original magnification: 400×, scale bar = 50 μm. ****$p < 0.0001$.

groups. Colon tissues in patients with UC exhibited higher levels of infiltrating activated B cells, activated CD4 and CD8 T cells, central memory CD4 T cells, effector memory CD8 T cells, immature dendritic cells, mast cells, myeloid-derived suppressor cells (MDSCs), neutrophils, and regulatory T cells compared to HC.

Further analysis of the relationship between immune cells and sene-DEGs revealed significant associations. ABCB1 showed the strongest correlation with central memory CD8 T cells and MDSCs (Figure 9D), while LCN2 was most strongly correlated with effector memory CD8 T cells and T follicular helper cells (Figure 9E).

Discussion

UC is a chronic, recurrent bowel disorder primarily marked by inflammation and ulceration of the colon and rectum, with an etiology that remains largely unclear and involves multifactorial inflammation.[2] Increasing evidence suggests that UC accelerates colon aging, evidenced by shortened telomeres in colonocytes, altered mRNA expression of telomere-binding proteins, and DNA damage,[10,15] highlighting the potential of senescence-related genes for predicting prognosis and treatment response. While inflammation and senescence are closely linked through the senescence-associated secretory phenotype, the precise molecular pathways that drive senescence-mediated immune infiltration in UC remain unclear. Investigating the association between senescence and UC may reveal novel prognostic markers, diagnostic indicators, and therapeutic targets and elucidate the underlying mechanisms of the disease.

In this study, 14 sene-DEGs were identified by overlapping the DEGs with senescence-related genes. Unsupervised clustering analysis based on the expression of these 14 sene-DEGs identified two senescence-related subtypes of UC. Subtype 1 exhibited significantly lower expression levels of signature genes compared to subtype 2. Notably, the immune cell infiltration in colonic tissue differed significantly between the subtypes, with subtype 1 showing higher levels of immune cell infiltration. Functional enrichment analyses revealed that subtype 2 was characterized by a higher prevalence of inflammatory pathways and a lower prevalence of metabolic pathways, whereas subtype 1 displayed the opposite pattern.

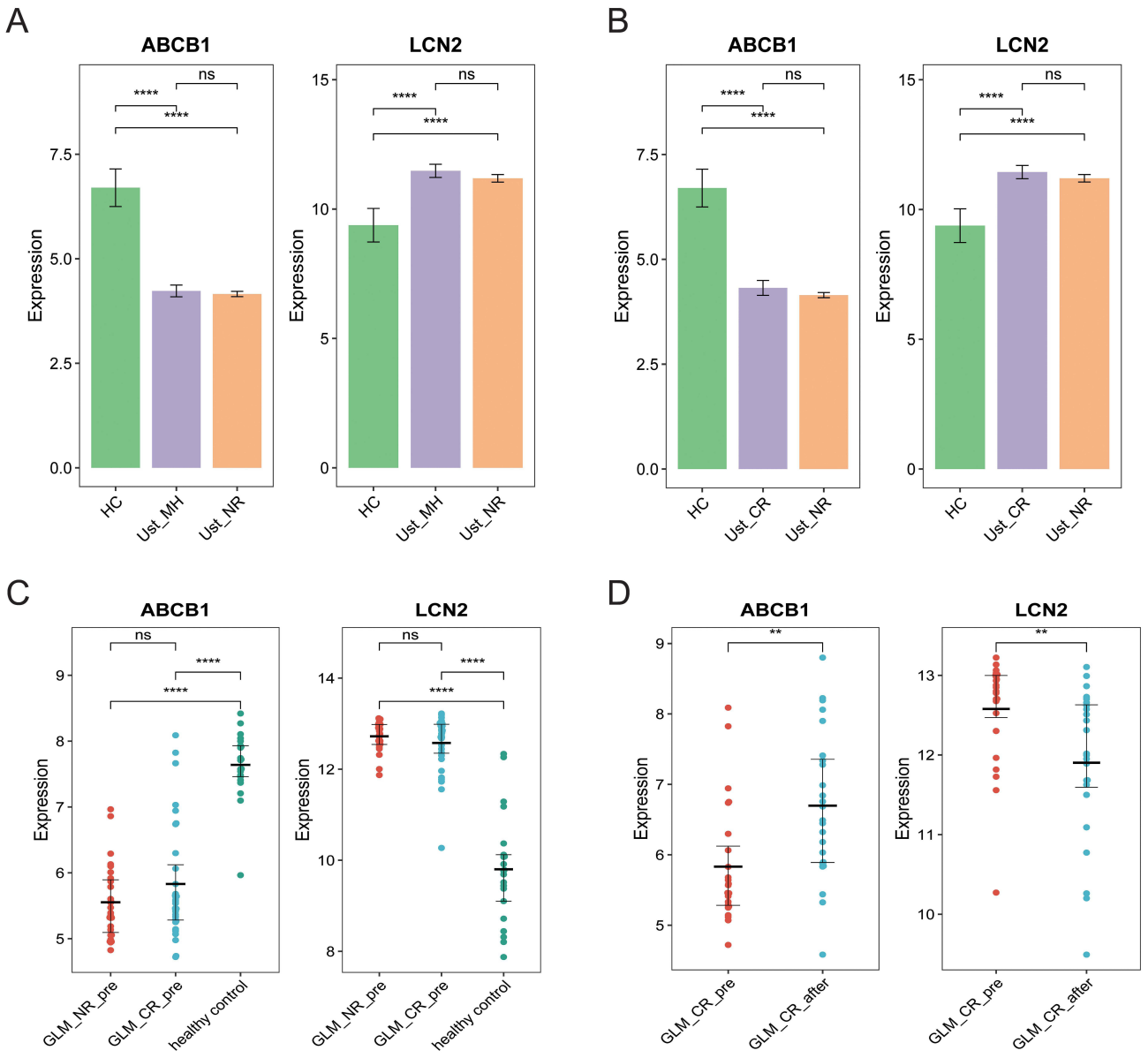

Figure 8 Expression levels of ABCB1 and LCN2 in colonic mucosa. (**A**) Relative expression levels of ABCB1 and LCN2 in the colonic mucosa of HC and patients with UC categorized by mucosal healing and non-response groups prior to Ust therapy. (**B**) Relative expression levels of ABCB1 and LCN2 in the colonic mucosa of HC and patients with UC classified as clinical responders and non-responders before Ust therapy. (**C** and **D**) Relative expression levels of ABCB1 and LCN2 in the colonic mucosa of HC and patients with UC categorized as responders and non-responders before and after GLM treatment. $^{**}p < 0.01$, $^{****}p < 0.0001$.
Abbreviations: ns, not statistically significant; Ust, ustekinumab; GLM, golimumab; MH, mucosal healing; CR, clinical response; NR, non-response.

Subtype 2 was associated with several key pathways, including the MAPK signaling pathway, JAK/STAT signaling pathway, ECM receptor interaction, and chemokine signaling pathway. These pathways are critically involved in UC pathogenesis, as dysregulation of proinflammatory and anti-inflammatory molecules plays a significant role. Notably, dysfunction and genetic variations in the JAK-STAT pathways have been identified as pivotal mechanisms in UC, with several JAK inhibitors like tofacitinib and filgotinib showing efficacy in recent UC treatments.[16,17] Additionally, Feng Y et al demonstrated that a novel polysaccharide mitigated DSS-induced colitis through modulation of the MAPK signaling pathway.[18] Conversely, subtype 1 was linked to metabolic pathways such as glycolysis, gluconeogenesis, pyruvate metabolism, propanoate metabolism, oxidative phosphorylation, fatty acid metabolism, limonene, and pinene degradation. These complex metabolic pathways are known to influence the inflammatory response of cells. Immune cells, including T cells, macrophages, dendritic cells, and NK cells, play critical roles in IBD pathogenesis.[19] Recent

https://doi.org/10.2147/JIR.S508396

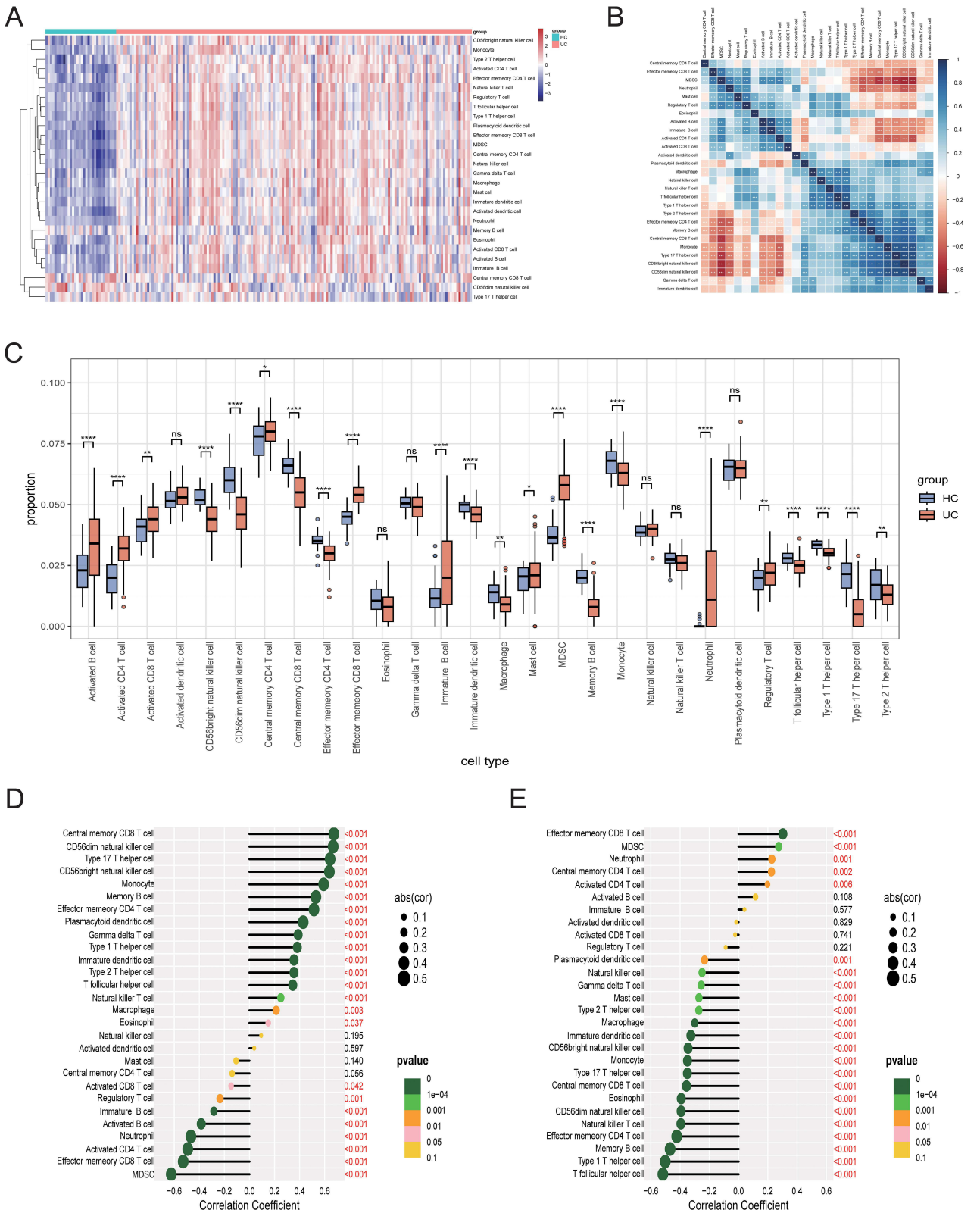

Figure 9 Immune cell infiltration and correlations in UC. (**A**) Heatmap depicting differences in immune cell infiltration in the colonic tissue between patients with UC and HC. (**B**) Heatmap illustrating the correlations among immune cells. (**C**) Differences in immune cell infiltration between patients with UC and HC. (**D** and **E**) Lollipop charts showing the correlation between ABCB1 (**D**) and LCN2 (**E**) expression and immune cells. *$p < 0.05$, **$p < 0.01$, ***$p < 0.001$, ****$p < 0.0001$.
Abbreviation: ns, not statistically significant.

research has shown that cyclosporine can alleviate severe ulcerative colitis by enhancing neutrophil glycolysis.[20] Thus, targeting senescence-related genes with new inhibitors or immunomodulators could offer innovative therapeutic approaches for UC. Overall, systematic studies on senescence subtypes and diagnostic markers in UC will deepen our understanding of the disease's pathogenesis and support the development of personalized diagnostic and treatment strategies.

Machine learning has gained significant attention for its effectiveness in clinical diagnosis. In this study, eight machine learning models were employed to identify senescence-related DEGs predictive of UC progression. LightGBM achieved the highest AUC value of 0.978, while AdaBoost demonstrated superior accuracy (0.8426), kappa (0.4894), and F1-score (0.9040). Among the 14 sene-DEGs, ABCB1 and LCN2 emerged as key biomarkers with strong diagnostic predictive capabilities for UC. The expression levels of these genes were validated in independent datasets and colon tissue samples from patients with UC and HC, confirming the consistency of experimental results with bioinformatics predictions.

ABCB1, also known as MDR1, encodes P-glycoprotein (P-gp), an ATP-dependent membrane transporter.[21] P-gp is highly expressed on the intestinal epithelial cell membrane, where it mediates the efflux of toxins, drugs, and harmful bacteria from the mucosa into the lumen, thereby maintaining intestinal homeostasis.[22] Reduced expression of P-gp in the colonic mucosa of patients with colitis has been documented,[23] and the P-gp expression was negatively correlated with the levels of IL-6 mRNA. Other studies also indicated ABCB1 knockout mice exhibit spontaneous colitis resembling human UC.[24,25] Furthermore, the expression of ABCB1 increases in $CD4^{+}CD8^{+}$T lymphocytes with age, indicating that P-gp may be involved in the secretion of cytokines, growth factors, and cytotoxic molecules.[26] Additionally, Foley SE et al identified a mechanistic link between gut microbiota and P-gp, noting that P-gp regulates gut microbiota to suppress excessive inflammation and sustain intestinal balance.[27]

LCN2, a 25 kDa secreted glycoprotein, functions as a transporter for lipophilic small molecules, including steroids, lipopolysaccharides, iron, and fatty acids.[26] Recent studies have highlighted LCN2 as an effector molecule in cGAS-STING-YY1 mediated astrocyte senescence in Parkinson's disease,[28] and shown that M1 macrophage-derived exosomes exacerbate nucleus pulposus cell senescence via the LCN2/NF-κB signaling pathway in intervertebral disc degeneration.[29] Furthermore, LCN2 plays a critical role in preventing gut microbiota dysbiosis-induced colitis.[30] In addition, silencing of LCN2 suppressed ferroptosis events in both in vivo and in vitro colitis model, demonstrating that LCN2 is also a key factor in regulating ferroptosis in UC.[31]

Our validation of sene-DEGs expression patterns across various datasets, comparing patients with UC with HC and lesion versus non-lesion groups, revealed significant differences. This underscores the role of senescence in UC progression. Notably, expression levels of sene-DEGs varied significantly between active and inactive phases of UC, suggesting that targeting senescence could potentially reduce UC recurrence.

Immune association analyses showed that ABCB1 was most strongly correlated with central memory CD8 T cells and MDSCs, while LCN2 exhibited the highest correlations with effector memory CD8 T cells and T follicular helper cells. CD8+ T cell-mediated adaptive immune responses play an important role in the fight against pathogenic microbial infections and tumors, as well as in the maintenance of tissue homeostasis.[32] Recent studies have emphasized the role of diminishing CD8+central memory T and CD8+resident memory T cells in psoriatic skin inflammation and its relapse.[33] It has been shown the gut microbiome can control accumulation of MDSCs in the liver in the context of colitis.[34] These findings suggest that ABCB1 and LCN2 may influence different UC subtypes through immune regulation, warranting further research into their role in UC development through gene integration and immune response.

The impact of biological agents on sene-DEGs further supports the critical role of senescence in UC progression. Significant reductions in sene-DEGs expression following treatment with biologics such as GLM and Ust highlight the relevance of senescence in UC management. Future research should continue to explore the relationship between senescence and UC development.

Overall, our study emphasizes the potential of senescence as a diagnostic and therapeutic target in UC. By examining senescence-related biomarkers and their roles in different UC subtypes, we provide a framework for developing targeted management strategies that may enhance the precision of UC treatment.

Conclusion

In conclusion, this study advances the understanding of cellular senescence-associated genes in UC pathogenesis, emphasizing the critical roles of ABCB1 and LCN2 in cellular senescence within UC.

Data Sharing Statement

These data were derived from the following resources available in the public domain: Gene Expression Omnibus (GEO) database (http://www.ncbi.nlm.nih.gov/geo). The corresponding author can be directed for further requirements.

Ethical Approval and Consent to Participate

The study adhered to the Declaration of Helsinki and was approved by the Ethics Committee of Renmin Hospital of Wuhan University (WDRY2021-K025). Informed consent was obtained from all patients, and the study was conducted in accordance with relevant guidelines and regulations.

Acknowledgment

The authors thank the National Cancer Institute for providing the Gene Expression Omnibus (GEO) data set. In addition, the authors would like to thank the editors and the anonymous reviewers for their valuable comments and suggestions to improve the quality of the paper.

Funding

This research was funded by the Natural Science Foundation of Hubei Province (No. 2022CFB703), the Key Laboratory Open Project of Hubei Province (No. 2021KFH015), the Key Laboratory Open Project of Hubei Province (No. 2022KFH029).

Disclosure

The authors report no conflicts of interest in this work.

References

1. Rivière P, Li Wai Suen C, Chaparro M, De Cruz P, Spinelli A, Laharie D. Acute severe ulcerative colitis management: unanswered questions and latest insights. *Lancet Gastroenterol Hepatol*. 2024;9(3):251–262. doi:10.1016/S2468-1253(23)00313-8
2. Le Berre C, Honap S, Peyrin-Biroulet L. Ulcerative colitis. *Lancet*. 2023;402(10401):571–584. doi:10.1016/S0140-6736(23)00966-2
3. Wu X, Wei S, Chen M, et al. P2RY13 exacerbates intestinal inflammation by damaging the intestinal mucosal barrier via activating IL-6/STAT3 pathway. *Int J Biol Sci*. 2022;18(13):5056–5069. doi:10.7150/ijbs.74304
4. Bopanna S, Ananthakrishnan AN, Kedia S, Yajnik V, Ahuja V. Risk of colorectal cancer in Asian patients with ulcerative colitis: a systematic review and meta-analysis. *Lancet Gastroenterol Hepatol*. 2017;2(4):269–276. doi:10.1016/S2468-1253(17)30004-3
5. Shah SC, Itzkowitz SH. Colorectal cancer in inflammatory bowel disease: mechanisms and management. *Gastroenterology*. 2022;162(3):715–730.e3. doi:10.1053/j.gastro.2021.10.035
6. Kobayashi T, Siegmund B, Le Berre C, et al. Ulcerative colitis. *Nat Rev Dis Primers*. 2020;6(1):74. doi:10.1038/s41572-020-0205-x
7. Amarnani A, Thakker S, Panush RS. Reflecting on the immunopathology of arthritis associated with inflammatory bowel disease: what do we know and what should we know? *Clin Rheumatol*. 2022;41(8):2581–2588. doi:10.1007/s10067-022-06201-3
8. Li X, Li C, Zhang W, Wang Y, Qian P, Huang H. Inflammation and aging: signaling pathways and intervention therapies. *Signal Transduct Target Ther*. 2023;8(1):239. doi:10.1038/s41392-023-01502-8
9. Sienkiewicz M, Sroka K, Binienda A, Jurk D, Fichna J. A new face of old cells: an overview about the role of senescence and telomeres in inflammatory bowel diseases. *Ageing Res Rev*. 2023;91:102083. doi:10.1016/j.arr.2023.102083
10. Risques RA, Lai LA, Brentnall TA, et al. Ulcerative colitis is a disease of accelerated colon aging: evidence from telomere attrition and DNA damage. *Gastroenterology*. 2008;135(2):410–418. doi:10.1053/j.gastro.2008.04.008
11. Watanabe S, Hibiya S, Katsukura N, et al. Importance of telomere shortening in the pathogenesis of ulcerative colitis: a new treatment from the aspect of telomeres in intestinal epithelial cells. *J Crohns Colitis*. 2022;16(1):109–121. doi:10.1093/ecco-jcc/jjab115
12. Yu G, Wang LG, Han Y, He QY. clusterProfiler: an R package for comparing biological themes among gene clusters. *OMICS*. 2012;16(5):284–287. doi:10.1089/omi.2011.0118
13. Markovich Gordon M, Moser AM, Rubin E. Unsupervised analysis of classical biomedical markers: robustness and medical relevance of patient clustering using bioinformatics tools. *PLoS One*. 2012;7(3):e29578. doi:10.1371/journal.pone.0029578
14. Hänzelmann S, Castelo R, Guinney J. GSVA: gene set variation analysis for microarray and RNA-seq data. *BMC Bioinf*. 2013;14(1):7. doi:10.1186/1471-2105-14-7
15. Da-Silva N, Arasaradnam R, Getliffe K, Sung E, Oo Y, Nwokolo C. Altered mRNA expression of telomere binding proteins (TPP1, POT1, RAP1, TRF1 and TRF2) in ulcerative colitis and Crohn's disease. *Dig Liver Dis*. 2010;42(8):544–548. doi:10.1016/j.dld.2009.12.005

16. Salas A, Hernandez-Rocha C, Duijvestein M, et al. JAK-STAT pathway targeting for the treatment of inflammatory bowel disease. *Nat Rev Gastroenterol Hepatol*. 2020;17(6):323–337. doi:10.1038/s41575-020-0273-0
17. Pérez-Jeldres T, Tyler CJ, Boyer JD, et al. Targeting cytokine signaling and lymphocyte traffic via small molecules in inflammatory bowel disease: JAK inhibitors and S1PR agonists. *Front Pharmacol*. 2019;10:212. doi:10.3389/fphar.2019.00212
18. Feng Y, Chen S, Song Y, et al. A novel Sagittaria sagittifolia L. polysaccharides mitigate DSS-induced colitis via modulation of gut microbiota and MAPK/NF-κB signaling pathways. *Int J Biol Macromol*. 2024;254(Pt 3):127835. doi:10.1016/j.ijbiomac.2023.127835
19. Zaiatz Bittencourt V, Jones F, Doherty G, Ryan EJ. Targeting immune cell metabolism in the treatment of inflammatory bowel disease. *Inflamm Bowel Dis*. 2021;27(10):1684–1693. doi:10.1093/ibd/izab024
20. Lu H, Lin J, Xu C, et al. Cyclosporine modulates neutrophil functions via the SIRT6-HIF-1α-glycolysis axis to alleviate severe ulcerative colitis. *Clin Transl Med*. 2021;11(2):e334. doi:10.1002/ctm2.334
21. Skinner KT, Palkar AM, Hong AL. Genetics of ABCB1 in Cancer. *Cancers*. 2023;15(17):4236. doi:10.3390/cancers15174236
22. Szabady RL, Louissaint C, Lubben A, et al. Intestinal P-glycoprotein exports endocannabinoids to prevent inflammation and maintain homeostasis. *J Clin Invest*. 2018;128(9):4044–4056. doi:10.1172/JCI96817
23. Englund G, Jacobson A, Rorsman F, Artursson P, Kindmark A, Rönnblom A. Efflux transporters in ulcerative colitis: decreased expression of BCRP (ABCG2) and Pgp (ABCB1). *Inflamm Bowel Dis*. 2007;13(3):291–297. doi:10.1002/ibd.20030
24. Resta-Lenert S, Smitham J, Barrett KE. Epithelial dysfunction associated with the development of colitis in conventionally housed mdr1a-/- mice. *Am J Physiol Gastrointest Liver Physiol*. 2005;289(1):G153–162. doi:10.1152/ajpgi.00395.2004
25. Wilk JN, Bilsborough J, Viney JL. The mdr1a-/- mouse model of spontaneous colitis: a relevant and appropriate animal model to study inflammatory bowel disease. *Immunol Res*. 2005;31(2):151–159. doi:10.1385/IR:31:2:151
26. Xiao X, Yeoh BS, Vijay-Kumar M. Lipocalin 2: an emerging player in iron homeostasis and inflammation. *Annu Rev Nutr*. 2017;37(1):103–130. doi:10.1146/annurev-nutr-071816-064559
27. Foley SE, Tuohy C, Dunford M, et al. Gut microbiota regulation of P-glycoprotein in the intestinal epithelium in maintenance of homeostasis. *Microbiome*. 2021;9(1):183. doi:10.1186/s40168-021-01137-3
28. Jiang SY, Tian T, Yao H, et al. The cGAS-STING-YY1 axis accelerates progression of neurodegeneration in a mouse model of Parkinson's disease via LCN2-dependent astrocyte senescence. *Cell Death Differ*. 2023;30(10):2280–2292. doi:10.1038/s41418-023-01216-y
29. Fan C, Wang W, Yu Z, et al. M1 macrophage-derived exosomes promote intervertebral disc degeneration by enhancing nucleus pulposus cell senescence through LCN2/NF-κB signaling axis. *J Nanobiotechnology*. 2024;22(1):301. doi:10.1186/s12951-024-02556-8
30. Singh V, Yeoh BS, Chassaing B, et al. Microbiota-inducible innate immune, siderophore binding protein lipocalin 2 is critical for intestinal homeostasis. *Cell Mol Gastroenterol Hepatol*. 2016;2(4):482–498.e6. doi:10.1016/j.jcmgh.2016.03.007
31. Deng L, He S, Li Y, et al. Identification of lipocalin 2 as a potential ferroptosis-related gene in ulcerative colitis. *Inflamm Bowel Dis*. 2023;29(9):1446–1457. doi:10.1093/ibd/izad050
32. Raynor JL, Collins N, Shi H, et al. CRISPR screens unveil nutrient-dependent lysosomal and mitochondrial nodes impacting intestinal tissue-resident memory CD8+ T cell formation. *Immunity*. 2024;57(11):2597–2614.e13. doi:10.1016/j.immuni.2024.09.013
33. Chen Y, Yan Y, Liu H, et al. Dihydroartemisinin ameliorates psoriatic skin inflammation and its relapse by diminishing CD8+ T-cell memory in wild-type and humanized mice. *Theranostics*. 2020;10(23):10466–10482. doi:10.7150/thno.45211
34. Zhang Q, Ma C, Duan Y, et al. Gut microbiome directs hepatocytes to recruit MDSCs and promote cholangiocarcinoma. *Cancer Discov*. 2021;11(5):1248–1267. doi:10.1158/2159-8290.CD-20-0304